Earthq Eng & Eng Vib (2013) 12: 569-576 **DOI**: 10.1007/s11803-013-0198-5

Transient analysis of 1D inhomogeneous media by dynamic inhomogeneous finite element method

Yang Zailin†, Wang Yao‡ and Hei Baoping‡

College of Aerospace and Civil Engineering, Harbin Engineering University, Harbin 150001, China

Abstract: The dynamic inhomogeneous finite element method is studied for use in the transient analysis of one-dimensional inhomogeneous media. The general formula of the inhomogeneous consistent mass matrix is established based on the shape function. In order to research the advantages of this method, it is compared with the general finite element method. A linear bar element is chosen for the discretization tests of material parameters with two fictitious distributions. And, a numerical example is solved to observe the differences in the results between these two methods. Some characteristics of the dynamic inhomogeneous finite element method that demonstrate its advantages are obtained through comparison with the general finite element method. It is found that the method can be used to solve elastic wave motion problems with a large element scale and a large number of iteration steps.

Keywords: inhomogeneous media; elastic wave; transient analysis; dynamic inhomogeneous finite element method; discretization

1 Introduction

Most natural substances, even man-made materials, are heterogeneous and inhomogeneous. With the development of science and technology, research about the behaviors of inhomogeneous media has become increasingly necessary. The dynamics of inhomogeneous media is an important research topic in this field.

Currently, the approaches to homogeneous media are highly developed and widely applied. For example, the general finite element method is based on the homogeneous media theory, where all of the material parameters are uniform in the element. In region Ω, all of the material parameters are assumed to be constant.

$$\begin{cases} E_\Omega = E_0 \\ \nu_\Omega = \nu_0 \\ \rho_\Omega = \rho_0 \end{cases} \tag{1}$$

where E_Ω, ν_Ω and ρ_Ω are the material parameters in region Ω. E_0, ν_0 and ρ_0 are all constant.

In order to study inhomogeneous media problems, where the material parameters are related to coordinates, the region Ω is divided into n pieces of homogeneous subregions in common.

$$\begin{cases} E_{\Omega_i} = \overline{E_i} \\ \nu_{\Omega_i} = \overline{\nu_i}, \quad 1 \le i \le n, \quad \sum_{i=1}^{n} \Omega_i = \Omega \\ \rho_{\Omega_i} = \overline{\rho_i} \end{cases} \tag{2}$$

where Ω_i is the subregion; $E_{\Omega_i}, \nu_{\Omega_i}$ and ρ_{Ω_i} are the material parameters of subregion Ω_i; and $\overline{E_i}$, $\overline{\nu_i}$ and $\overline{\rho_i}$ are the equivalent constant material parameters in subregion Ω_i.

The approaches of homogeneous media can be used to compute and analyze inhomogeneous models after the above division and homogenization operations have been carried out.

As the difficulty can be greatly decreased by the processed model, these operations have been widely applied to inhomogeneous media mechanics, especially dynamics (Tarau and Otugen, 2002; Pei and Mu, 2003; Luo *et al.*, 2004; Fu *et al.*, 2010). However, in a continuous transitional inhomogeneous zone, the processed model is sometimes too different from the original problem, so that the resulting precision may be questionable. In order to improve the precision of the results, inordinate amounts of computing resources are needed. Even so, the results may still lack precision.

Correspondence to: Yang Zailin, College of Aerospace and Civil Engineering, Harbin Engineering University, Harbin 150001, China
Tel: +86-13945015652; Fax: +86-451-82519210
E-mail: yangzailin00@163.com
†Professor; ‡Lecture

Supported by: the Fundamental Research Funds for the Central Universities under Grant No. HEUCFZ1125, and the National Natural Science Foundation of China under Grant No. 10972064
Received September 17, 2012; **Accepted** April 17, 2013

Accordingly, several different methods have been established. Two special methods are of interest here, namely the exact element method and the inhomogeneous finite element method.

In 1992, Ji (1992) presented the exact element method for constructing finite elements to solve the bending of an inhomogeneous thin plate, and achieved a high precision. As there are only nine particular solutions in total for the analytic solutions of the inhomogeneous media wave motion (Yang and Chen, 2007), it is very difficult to widely use the exact element method in this field.

The inhomogeneous finite element method was established in 1985 (Zhang and Leech, 1985; 1987). The stiffness matrix of the finite element is modified by the inhomogeneous elastic matrix. The inhomogeneous isoparametric element has been introduced to composites for accurate static stress analysis. Li and Zou (1998) analyzed a static problem of functionally graded materials based on the inhomogeneous isoparametric element. Compared with the general finite element method, their results have greater precision and more smoothness with the same number of elements. Thus, the computational scale can be greatly decreased by this element with the same accuracy. Zhao *et al.* (2002) obtained great success in the fracture of functionally graded material by the inhomogeneous finite element method. Thus far, this method has mainly been used in static analysis, and only the stiffness matrix has been constructed.

In this study, the inhomogeneous finite element method is developed for dynamic analysis. The mass matrix of an inhomogeneous finite element is constructed, so it can now be used to achieve the transient response of inhomogeneous media. A numerical example is solved by the dynamic inhomogeneous finite element method. The results are compared with those obtained by the general finite element method, and demonstrate the many advantages of the dynamic inhomogeneous finite element method.

2 General finite element

2.1 Governing equations

Assume that the deformation is small enough. The strain of elasticity can be written as the derivative of displacement in the following form.

$$\boldsymbol{\varepsilon} = \boldsymbol{L}\boldsymbol{u} \tag{3}$$

where $\boldsymbol{u}$ is the displacement vector of elasticity; and $\boldsymbol{L}$ is the differential operator. They are expressed as follows.

$$\boldsymbol{u} = \begin{Bmatrix} u \\ v \\ w \end{Bmatrix} \tag{4}$$

$$\boldsymbol{L} = \begin{bmatrix} \partial/\partial x & 0 & 0 \\ 0 & \partial/\partial y & 0 \\ 0 & 0 & \partial/\partial z \\ 0 & \partial/\partial z & \partial/\partial y \\ \partial/\partial z & 0 & \partial/\partial x \\ \partial/\partial y & \partial/\partial x & 0 \end{bmatrix} \tag{5}$$

In generalized Hooke's law, the stress-strain relationship is described as the following form.

$$\boldsymbol{\sigma} = \boldsymbol{D}\boldsymbol{\varepsilon} = \boldsymbol{D}\boldsymbol{L}\boldsymbol{u} \tag{6}$$

Considering the equilibrium conditions of force, the equilibrium equation of 3D elastodynamics can be given in the absence of damping.

$$\boldsymbol{L}^{\mathrm{T}}\boldsymbol{D}\boldsymbol{L}\boldsymbol{u} + \boldsymbol{b} = \rho\ddot{\boldsymbol{u}} \tag{7}$$

There are two types of material parameters in Eq. (7): elastic coefficients and inertia coefficients. Elastic modulus and Poisson's ratio are two commonly used elastic coefficients. The structural stiffness can be affected by these coefficients. In the case of no damping, only the density of the inertia coefficient is of interest.

To obtain the solution for an elastodynamics problem, Eq. (7) is solved with the given boundary conditions and the given initial conditions.

2.2 Stiffness matrix and mass matrix

Assume that the displacement field $\boldsymbol{u}$ is in the following form.

$$\boldsymbol{u} = \boldsymbol{N}\boldsymbol{a}^{\mathrm{e}} \tag{8}$$

where $\boldsymbol{N}$ is the shape function matrix, and $\boldsymbol{a}^{\mathrm{e}}$ is the nodal displacement vector of the element.

By the Galerkin method, the dynamic equilibrium equation of every finite element can be conducted in the following form from Eq. (7).

$$\boldsymbol{k}\boldsymbol{a} + \boldsymbol{m}\ddot{\boldsymbol{a}} = \boldsymbol{r}(t) \tag{9}$$

where $\boldsymbol{k}$ is the element stiffness matrix; $\boldsymbol{m}$ is the element mass matrix; $\boldsymbol{a}$ is the nodal displacement vector of the element; $\ddot{\boldsymbol{a}}$ is the nodal acceleration vector of the element; and $\boldsymbol{r}(t)$ is the body force vector of the element.

Equation (10) is the expression of $\boldsymbol{k}$. Equation (11) is the expression of $\boldsymbol{m}$, and gives the formula of the consistent mass matrix.

$$\boldsymbol{k} = \oint_{\Omega_{\mathrm{e}}} (\boldsymbol{L}\boldsymbol{N})^{\mathrm{T}}\boldsymbol{D}(\boldsymbol{L}\boldsymbol{N})\mathrm{d}\Omega_{\mathrm{e}} \tag{10}$$

$$\boldsymbol{m} = \oint_{\Omega_{\mathrm{e}}} \boldsymbol{N}^{\mathrm{T}}\rho\boldsymbol{N}\mathrm{d}\Omega_{\mathrm{e}} \tag{11}$$

Considering a one-dimensional linear bar element, Eq. (12) is its stiffness matrix, and Eq. (13) is its

consistent mass matrix.

$$\boldsymbol{k}=\frac{EA}{L}\begin{bmatrix}1 & -1\\ -1 & 1\end{bmatrix} \tag{12}$$

$$\boldsymbol{m}=\frac{\rho AL}{6}\begin{bmatrix}2 & 1\\ 1 & 2\end{bmatrix} \tag{13}$$

Because all the material parameters are constant in the matrix, it is apparent that the general finite element method relies on homogeneous media theory.

3 Inhomogeneous finite element

3.1 Stiffness matrix and mass matrix

The inhomogeneous finite element can be constructed by introducing the shape function for interpretation. The material parameters are not uniform in the element, but follow a determinate form of distribution.

The distributions of material parameters are expressed as the form of approximated polynomial.

$$\begin{cases}E(x,y,z)=\boldsymbol{N}\mathbf{E}^{\mathrm{e}}\\ \nu(x,y,z)=\boldsymbol{N}\boldsymbol{\nu}^{\mathrm{e}}\\ \rho(x,y,z)=\boldsymbol{N}\boldsymbol{\rho}^{\mathrm{e}}\end{cases} \tag{14}$$

where $\boldsymbol{E}^{\mathrm{e}}$ is the nodal elastic modulus array; $\boldsymbol{V}^{\mathrm{e}}$ is the nodal Poisson's ratio array; and $\boldsymbol{\rho}^{\mathrm{e}}$ is the nodal density array.

Similar to the general finite element, the element stiffness matrix and element mass matrix of the inhomogeneous finite element can be given as follows by using the Galerkin method.

$$\boldsymbol{k}=\oint_{\Omega_{\mathrm{e}}}(\boldsymbol{LN})^{\mathrm{T}}\boldsymbol{D}'(\boldsymbol{LN})\mathrm{d}\Omega_{\mathrm{e}} \tag{15}$$

$$\boldsymbol{m}=\oint_{\Omega_{\mathrm{e}}}\boldsymbol{N}^{\mathrm{T}}\boldsymbol{\Upsilon}\boldsymbol{N}\mathrm{d}\Omega_{\mathrm{e}} \tag{16}$$

Considering a one-dimensional linear bar element, Eq. (17) is its stiffness matrix, and Eq. (18) is its consistent mass matrix.

$$\boldsymbol{k}=\frac{A(E_1+E_2)}{2L}\begin{bmatrix}1 & -1\\ -1 & 1\end{bmatrix} \tag{17}$$

$$\boldsymbol{m}=\frac{AL}{12}\begin{bmatrix}3\rho_1+\rho_2 & \rho_1+\rho_2\\ \rho_1+\rho_2 & \rho_1+3\rho_2\end{bmatrix} \tag{18}$$

where E_1 and E_2 are the nodal elastic modulus, and ρ_1 and ρ_2 are the nodal density.

Obviously, the inhomogeneous stiffness matrix and inhomogeneous mass matrix all are symmetric. In addition, if the nodal values of each parameter are equal, Eqs. (17) and (18) transform to Eqs. (12) and (13).

3.2 Discretization test of parameter

In order to discuss the errors in parameter distribution introduced by different methods, a discretization test of the parameters has been done to compare the effect of discretization.

Two fictitious distributions as follows are used to express the heterogeneity of the material parameter of one-dimensional media.

$$P(x)=400x^2+1000 \quad (0\le x\le 1) \tag{19}$$

$$P(x)=\mathrm{e}^{-160(x-0.3)^2}+2\mathrm{e}^{-90(x-0.7)^2}+5 \ \ (0\le x\le 1) \tag{20}$$

The linear bar element is chosen for discretization. The model is divided into 20 elements with the same length. The densities of every general finite element are obtained based on the coordinate of element centroid. And the nodal densities of every inhomogeneous finite element are obtained based on the nodal coordinate.

The effect of discretization is shown in Figs. 1(a) and 1(b). Through these curves, it is seen that there are more errors between the actual distribution and the discrete results obtained by the general finite element method.

For example, the distribution of the parameters in Case 1 is a typical parabola. The error amplitude of

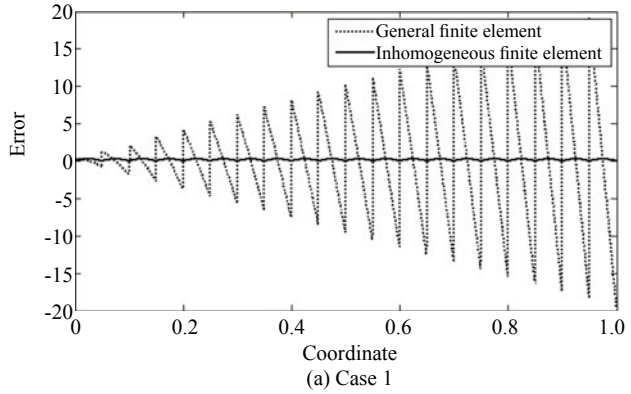

(a) Case 1

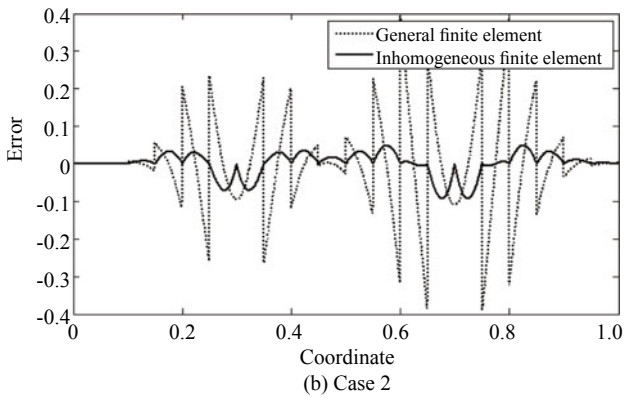

(b) Case 2

Fig. 1 Effect of discretization

the general finite element is about 20. However, the error of the inhomogeneous finite element is almost 0, and can even be ignored. Of course, if the quadratic bar element is chosen for discretization, the error of the inhomogeneous finite element is 0. Then, the distribution of the parameters in Case 2 is a combination of two Gaussian functions. The error amplitude of the general finite element is about 0.4; however, the error of the inhomogeneous finite element is less than 0.1.

From a sensory point of view, the general finite element brings more errors into the finite element model than the inhomogeneous finite element. Actually, the model error is finally decided by integration (Eqs. (10) and (11); Eqs. (15) and (16)). Of course, the general finite element still brings more errors. If the quadratic element or higher order element is chosen for discretization, there will be much better performance with the errors introduced by the inhomogeneous finite element. Thus, it is better to use the inhomogeneous finite element for discretization when dealing with the problem of inhomogeneous media.

4 Numerical example

In order to verify the advantages of the dynamic inhomogeneous finite element method, a numerical example is used for simulation and analysis.

4.1 Model description

There are two layers in this model as shown in Fig. 2(a). Layer B is a semi-infinite medium covered with the vertical inhomogeneous Layer A, and the upper surface is free. Layer A is infinite in the horizontal direction.

The thickness of Layer A is 1. Assume that Layer B can be regarded as a rigid wall, so the lower surface of layer A is bounded. The material parameters are defined as follows.

$$\begin{cases} E(x) = E_0(1 - a_1(x-1) + b_1(x-1)^2) \\ \rho(x) = \rho_0(1 - a_2(x-1) + b_2(x-1)^2) \end{cases} \tag{21}$$

where

$$\begin{aligned} E_0 &= 13.3\times10^9 \\ a_1 &= 0.1 \\ b_1 &= 0.05 \\ \rho_0 &= 2500 \\ a_2 &= 0.2 \\ b_2 &= 0.07 \end{aligned}$$

If the upper surface of Layer A is subjected to a uniform vertical impact load Q, a series of responses can be generated in this layer. The displacement field ($0 \le T \le 0.5$) in Layer A and the displacement history curve at the central section are solved and analyzed.

The original model is then simplified according to the known conditions. The simplified 1D model is shown in Fig. 2(b). The impact force is defined as follows.

$$F(t) = \begin{cases} 1000 & 0 \le t \le 4\times10^{-7} \\ 0 & t > 4\times10^{-7} \end{cases} \tag{22}$$

4.2 Results

To solve this problem, the linear bar element is chosen for the finite element analysis. This model is divided into 50, 100, 200 and 400 elements with the same element length. Then, the Newmark Method is used to solve these cases. The results are described in the following paragraphs.

The dynamic inhomogeneous finite element method has a good convergence as seen in Fig. 3 and Fig. 4. And, the dynamic behavior of inhomogeneous media looks very different from homogeneous media.

4.3 Comparison

There is an apparent difference in the stiffness matrix and mass matrix between the general finite element and inhomogeneous finite element methods. To observe the advantages of the dynamic inhomogeneous finite element method, a comparison was carried out using the same conditions. The resulting differences between the dynamic inhomogeneous finite element and general finite element methods are shown in Figs. 5 and 6.

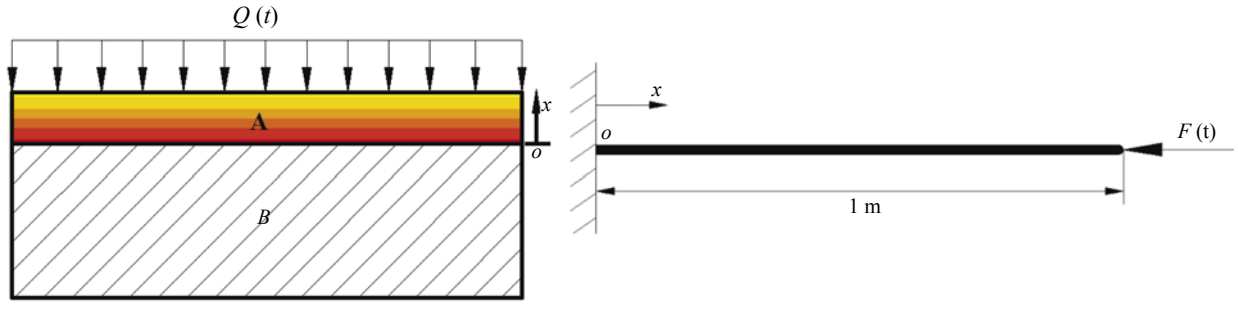

(a) Original model (b) Simplified model

Fig. 2 Modeling

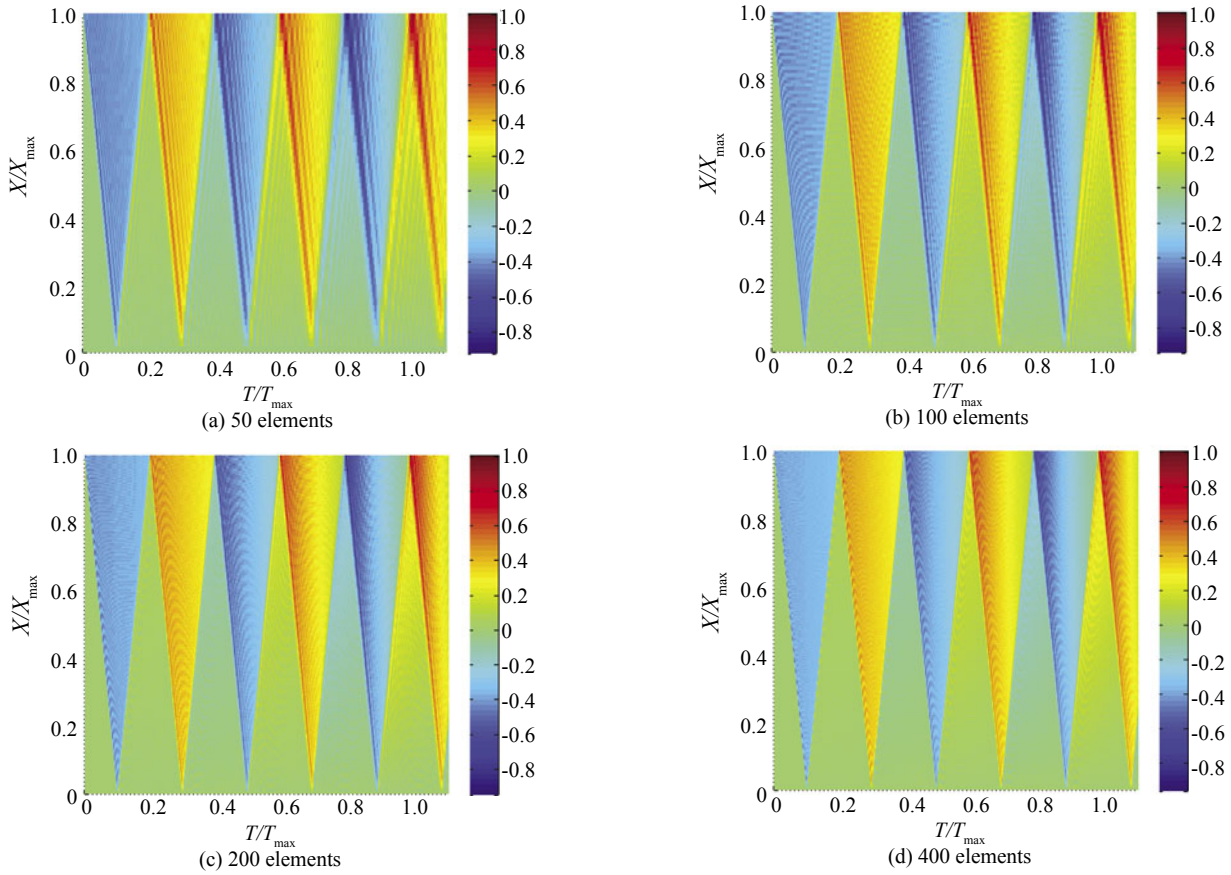

Fig. 3 Displacement field ($0 \le T \le 0.5$) in Layer A

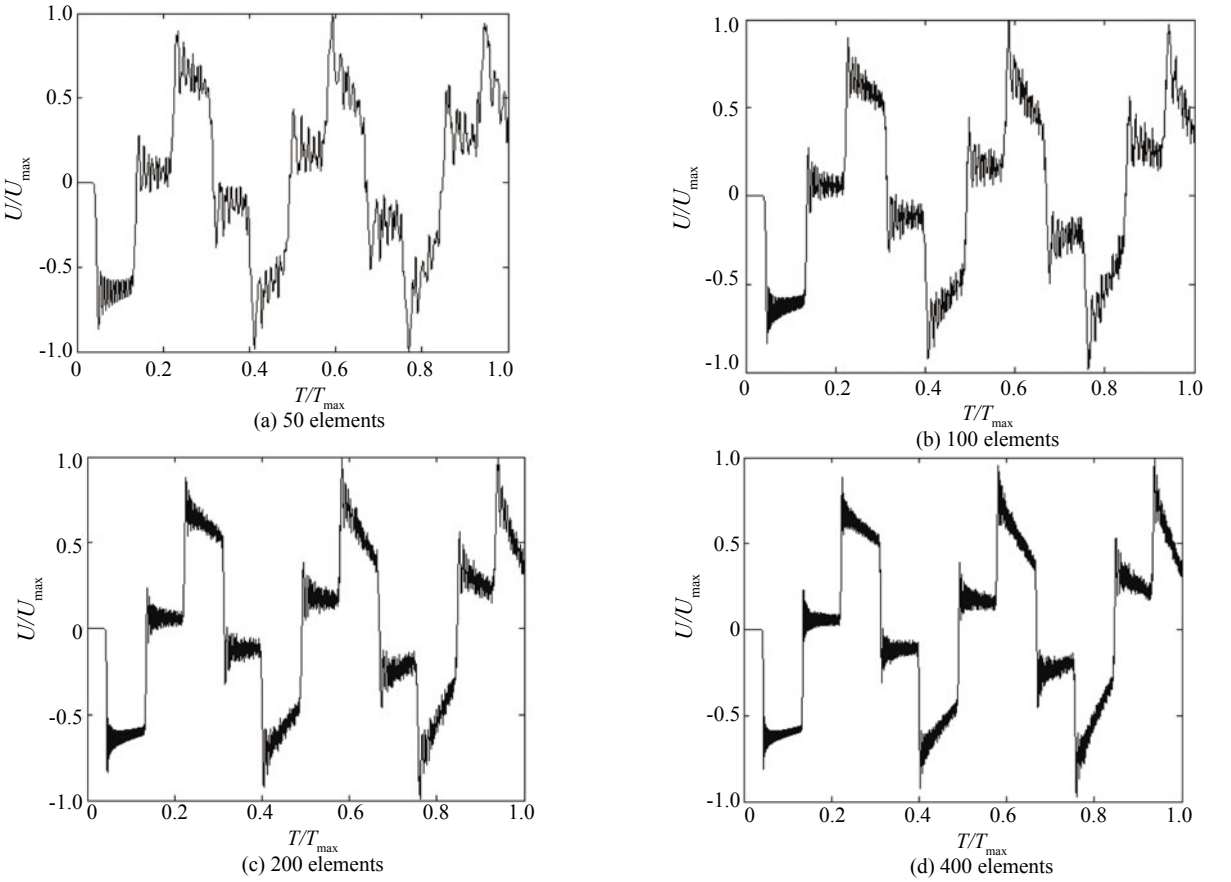

Fig. 4 Displacement history curve ($0 \le T \le 0.5$) at the central section

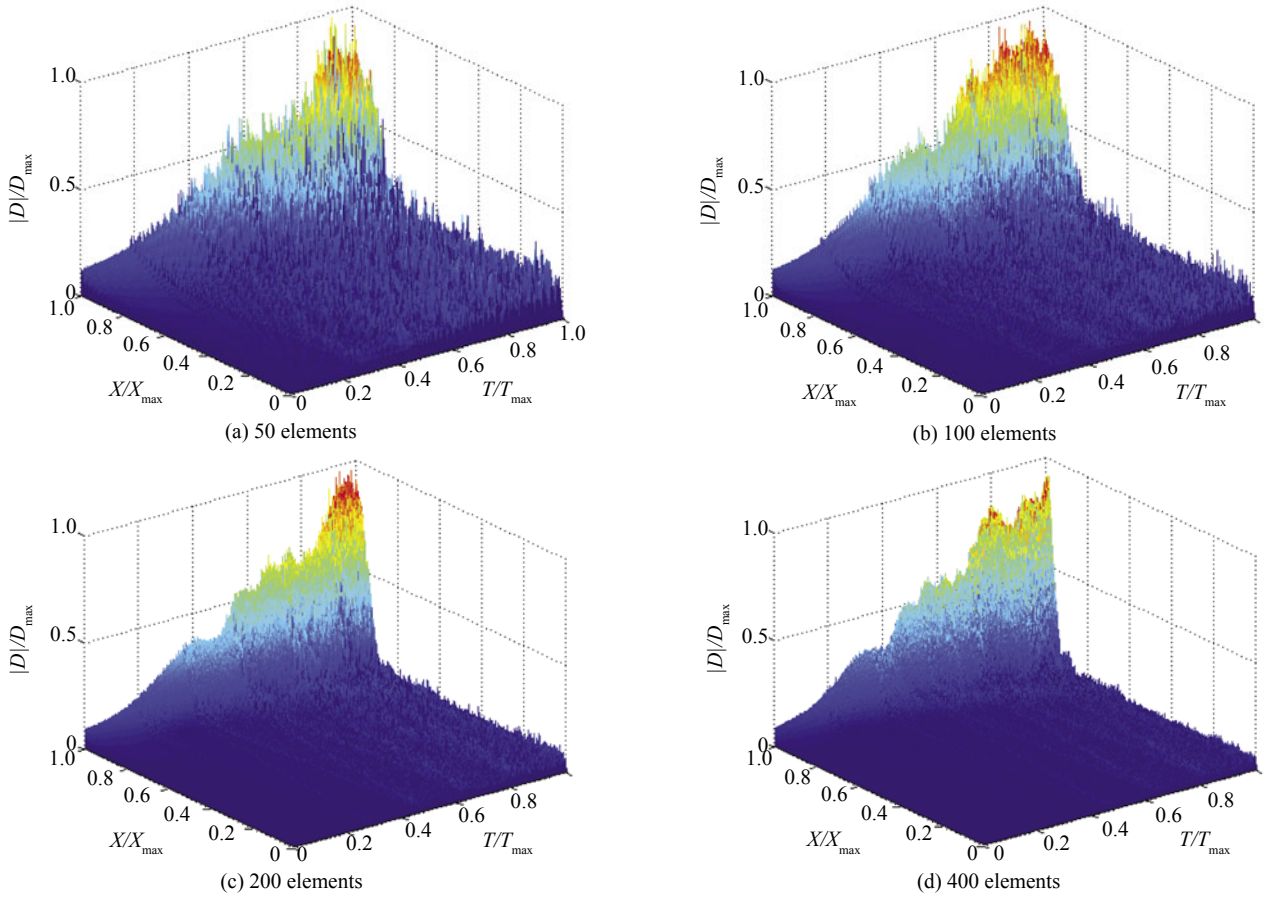

Fig. 5 Difference in the displacement field ($0 \le T \le 0.5$) of Layer A

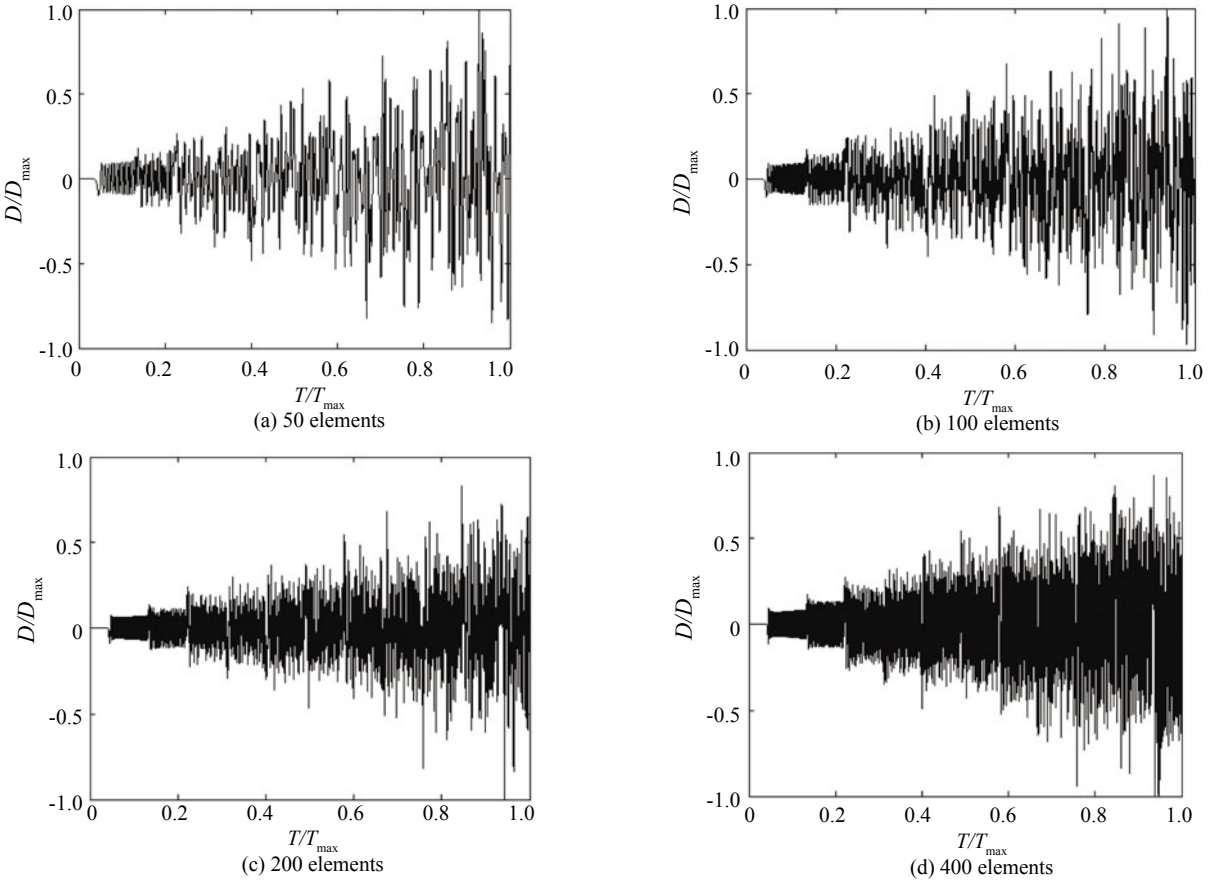

Fig. 6 Difference in the displacement history curve ($0 \le T \le 0.5$) at the central section

Three characteristics can be observed from these differences.

First, the difference of the nodal displacement at the free end is obviously larger than those at the other positions.

Second, the difference in the nodal displacements increases with iteration step by step. On the one hand, the resulting difference increases slowly and approximately linearly in the same step. On the other hand, the resulting difference suddenly lifts to a larger amplitude when the wave front arrives.

Third, the resulting difference decreases as the element number increases (see Table 1). This is a typical feature of the finite element method.

Table 1 Maximum differences of displacement in Figs. 5 and 6

Number	$D_{\max}$(Fig. 5) (10^{-17})	$D_{\max}$(Fig. 6) (10^{-17})
50	18.20	4.44
100	9.32	1.69
200	6.20	0.798
400	3.36	0.237

The first characteristic is caused by the difference in the stiffness and mass matrices. Since the stiffness and mass related to the constrained node are meaningless to the process of solving the finite element equation, only unconstrained nodes need to be taken into account.

Through the dynamic inhomogeneous finite element method, the element values of the assembled mass matrix associated with node m at the free end and internal node n are as follows.

$$\boldsymbol{m}_m = \frac{AL}{12}\begin{bmatrix} \rho_{m-1}+\rho_m & \\ \rho_{m-1}+\rho_m & \rho_{m-1}+3\rho_m \end{bmatrix} \tag{23}$$

$$\boldsymbol{m}_n = \frac{AL}{12}\begin{bmatrix} & \rho_{n-1}+\rho_n & \\ \rho_{n-1}+\rho_n & \rho_{n-1}+6\rho_n+\rho_{n+1} & \rho_n+\rho_{n+1} \\ & \rho_n+\rho_{n+1} & \end{bmatrix} \tag{24}$$

By using the general finite element method, the coefficients of the assembled mass matrix associated with the free end node m and internal node n are as follows.

$$\boldsymbol{m}_m' = \frac{AL}{6}\begin{bmatrix} & \rho_{m-0.5} \\ \rho_{m-0.5} & 2\rho_{m-0.5} \end{bmatrix} \tag{25}$$

$$\boldsymbol{m}_n' = \frac{AL}{6}\begin{bmatrix} & \rho_{n-0.5} & \\ \rho_{n-0.5} & 2(\rho_{n-0.5}+\rho_{n+0.5}) & \rho_{n+0.5} \\ & \rho_{n+0.5} & \end{bmatrix} \tag{26}$$

Thus, the differences seen in the mass matrix coefficients by these two different methods are given as follows.

$$\boldsymbol{m}_m - \boldsymbol{m}_m' = \frac{AL}{12}\begin{bmatrix} & D_1 \\ D_1 & D_2 \end{bmatrix} \tag{27}$$

$$\boldsymbol{m}_n - \boldsymbol{m}_n' = \frac{AL}{12}\begin{bmatrix} & D_3 & \\ D_3 & D_4 & D_5 \\ & D_5 & \end{bmatrix} \tag{28}$$

$$D_1 = \rho_{m-1} + \rho_m - 2\rho_{m-0.5}$$
$$D_2 = \rho_{m-1} + 3\rho_m - 4\rho_{m-0.5}$$
$$D_3 = \rho_{n-1} + \rho_n - 2\rho_{n-0.5}$$
$$D_4 = \boldsymbol{\rho}_{n-1} + \rho_{n+1} + 6\rho_n - 4(\rho_{n-0.5} + \rho_{n+0.5})$$
$$D_5 = \rho_n + \rho_{n+1} - 2\rho_{n+0.5}$$

Substituting Eq. (21) for the material parameter in Eqs. (27) and (28) gives

$$\boldsymbol{m}_m - \boldsymbol{m}_m' = \frac{\rho_0 AL^2}{2400}\begin{bmatrix} & 7L \\ 7L & -40 \end{bmatrix} \tag{29}$$

$$\boldsymbol{m}_n - \boldsymbol{m}_n' = \frac{7\rho_0 AL^3}{2400}\begin{bmatrix} & 1 & \\ 1 & 0 & 1 \\ & 1 & \end{bmatrix} \tag{30}$$

where L is the length of the linear bar element.

In addition, the differences of the stiffness matrix coefficients associated to free end node m and internal node n are given as follows.

$$\boldsymbol{k}_m - \boldsymbol{k}_m' = \frac{E_0 AL}{80}\begin{bmatrix} & -1 \\ -1 & 1 \end{bmatrix} \tag{31}$$

$$\boldsymbol{k}_n - \boldsymbol{k}_n' = \frac{E_0 AL}{80}\begin{bmatrix} & -1 & \\ -1 & 2 & -1 \\ & -1 & \end{bmatrix} \tag{32}$$

The length of the bar element is far less than 1, so the nodal stiffness differences are very small, and are uniformly distributed in the discrete model in this example. Then, the nodal mass differences of the internal nodes are small, and are also uniformly distributed. However, the nodal mass difference at the free end is larger than at the other position. This larger mass difference leads to the first observed characteristic.

The second characteristic is also caused by the differences of the assembled stiffness and mass matrices. As the time increases, the differences in the results continually accumulate and gradually enlarge. And, a step appears when the wave front arrives. In addition, the wave front propagates back at the free end node, where the associated difference of the mass coefficient is largest. Therefore, these two reasons together lead to the increased difference with iteration step by step.

5 Conclusions

Several conclusions can be obtained from the results of this study.

First, the dynamic inhomogeneous finite element method proposed herein can be used to solve the large element scale of the discrete model. In the same conditions, it is more accurate than the general finite element method when the element scale of the model is very large, such as in crustal structure analysis. Certainly, the results of these two methods can be close or even almost the same when the element scale of the model is small enough.

Second, it is found that as the number of iterative steps increase, the advantages of the dynamic inhomogeneous finite element method also increases. Because the dynamic inhomogeneous finite element is superior in discretization effect, this method can be used to improve the resulting reliability of transient analysis with a long time history or a large number of iterative steps.

The inhomogeneous finite element method has been extended to solve dynamics problems in this study, and a high degree of accuracy and high efficiency has been obtained. This method can be expanded into 2D problems, 3D problems and axisymmetric problems. Hence, this achievement can be valuable in engineering applications and further research.

Acknowledgement

The authors gratefully acknowledge the financial support for this study provided by the Fundamental Research Funds for the Central Universities under Grant No. HEUCFZ1125 and the National Natural Science Foundation of China under Grant No. 10972064.

References

Fu Wen-hua, Jin Tao and Tian Xiao-pei (2010), "A Finite Element Model of Sound Propagation in Regions with Non-Uniform Temperature," *Journal of Fudan University*, **49**(1): 133–136. (in Chinese)

Ji Zhenyi (1992), "An Exact element Method for Bending of Nonhomogeneous Thin Plates," *Applied Mathematics and Mechanics*, **13**(8): 683–690.

Li Chunyu and Zou Zhenzhu (1998), "Finite Element Method for Nonhomogeneous Medium," *Mechanics in Engineering*, **20**(6): 10–12. (in Chinese)

Luo Songnan, Zhou Zhengping and Xiong Huier (2004), "Wave Transmission in a Continuous Transitional Inhomogeneous Zone," *Journal of Hunan University*, **31**(2): 97–100. (in Chinese)

Pei Zhenglin and Mu Yongguang (2003), "A Staggered-Grid High-order Difference Method for Modeling Seismic Wave Propagation in Inhomogeneous Media," *Journal of the University of Petroleum*, **27**(6): 17–21. (in Chinese)

Tarau C and Otugen MV (2002), "Propagation of Acoustic Waves through Regions of Non-uniform Temperature," *Aeroacoutics*, **1**(2): 165–181.

Yang Xunren and Chen Yu (2007), *Atmospheric Acoustics* 3rd ed, Beijing: Science Press. (in Chinese)

Zhang Shuangyin and Leech CM (1985), "Use of Inhomogeneous Finite Elements for the Prediction of Stress in Rope Terminations," *Engineering Computations*, **2**(1): 55–62.

Zhang Shuangyin and Leech CM (1987), "Inhomogeneous Isoparametric Elements for Stress Analysis of Composites," *Scientia Sinica*, **8**(XXX): 832–845.

Zhao Xishu, Zhang Shuangyin and WU Yongli (2002), "An Anaysis of a Crack in Functionally Gradient Coatings By Inhomogeneous Finite Element," *Engineering Mechanics*, **19**(4): 118–122. (in Chinese)